Energy & Environmental Science

Accepted Manuscript

This is an *Accepted Manuscript*, which has been through the Royal Society of Chemistry peer review process and has been accepted for publication.

Accepted Manuscripts are published online shortly after acceptance, before technical editing, formatting and proof reading. Using this free service, authors can make their results available to the community, in citable form, before we publish the edited article. We will replace this *Accepted Manuscript* with the edited and formatted *Advance Article* as soon as it is available.

You can find more information about *Accepted Manuscripts* in the Information for Authors.

Please note that technical editing may introduce minor changes to the text and/or graphics, which may alter content. The journal's standard Terms & Conditions and the Ethical guidelines still apply. In no event shall the Royal Society of Chemistry be held responsible for any errors or omissions in this *Accepted Manuscript* or any consequences arising from the use of any information it contains.

ROYAL SOCIETY OF CHEMISTRY

www.rsc.org/ees

Journal Name

RSCPublishing

ARTICLE

Direct Observation of an Inhomogeneous Chlorine Distribution in $CH_3NH_3PbI_{3-x}Cl_x$ Layers: Surface Depletion and Interface Enrichment

Cite this: DOI: 10.1039/xoxxoooooox

Received ooth January 2012,
Accepted ooth January 2012

DOI: 10.1039/xoxxoooooox

www.rsc.org/

David E. Starr,[a,*] Golnaz Sadoughi,[b] Evelyn Handick,[a] Regan G. Wilks,[a,c] Jan-Hendrik Alsmeier,[a] Leonard Köhler,[a] Mihaela Gorgoi,[d] Henry Snaith,[b,*] and Marcus Bär[a,c,e]

We have used hard X-ray photoelectron spectroscopy (HAXPES) at different photon energies and fluorescence yield X-ray absorption spectroscopy (FY-XAS) to non-destructively investigate $CH_3NH_3PbI_{3-x}Cl_x$ perovskite thin films on compact TiO_2. This combination of spectroscopic techniques allows the variation of information depth from the perovskite layer surface to the top-most part of the underlying compact TiO_2 layer. We have taken advantage of this to understand the distribution of chlorine throughout the perovskite/TiO_2 layer stack. No Cl is detected using HAXPES, indicating surface depletion of Cl and allowing us to place an upper limit on the amount of Cl in the perovskite layer: $x < 0.07$ and $x < 0.40$ to depths of ~10 nm and ~26 nm, respectively, beneath the perovskite film surface. Our FY-XAS results, however, demonstrate that there is a higher average concentration of Cl throughout the perovskite layer than at the surface ($x > 0.40$) consistent with both enhanced concentrations of Cl deep beneath the perovskite film surface and near the $CH_3NH_3PbI_{3-x}Cl_x$ perovskite/TiO_2 interface. The consequences of this distribution of Cl in the $CH_3NH_3PbI_{3-x}Cl_x$ perovskite layer on device performance are discussed.

Introduction

The most common technology currently used to directly convert sunlight into electricity is crystalline silicon-based (c-Si) solar cells.[1,2] Recently, a decline in the cost of c-Si-based solar cells has allowed solar energy to economically compete with fossil fuels for electricity generation in some parts of the world.[3] Whether the current cost of c-Si solar cells or rate of cost decrease is sustainable, however, remains an open question. This has led to increased research and development efforts in alternative solar cell technologies that may lead to further cost reductions or efficiency enhancement and the concomitant wider adoption of solar energy production.

Thin-film solar cell technologies promise to maintain or even increase the rate of cost reduction of solar cell production.[4] Among the emerging thin-film solar cell technologies, solution processed, organic-inorganic perovskite thin film-based solar cells have recently demonstrated dramatic increases in power conversion efficiency with values reaching 20.1 % within a few years.[5,6,7] Such cells portend to combine low-cost, solution-based production with high efficiency.[8] To date, high efficiencies have been reported for devices with methyl ammonium organometallic halide perovskites absorber layers, in particular $CH_3NH_3PbI_3$ and $CH_3NH_3PbI_{3-x}Cl_x$. A variety of deposition methods have been used to produce the perovskite layers, and numerous device configurations have been used.[6,9–12] In this paper we focus on understanding the chemical composition of $CH_3NH_3PbI_{3-x}Cl_x$ absorber layers and, in particular, the distribution of Cl throughout the layer.

The performance of $CH_3NH_3PbI_{3-x}Cl_x$ based solar cells strongly depends on processing parameters.[13,14] Interestingly, spectroscopic studies of $CH_3NH_3PbI_{3-x}Cl_x$ layers indicate that the layers are deficient in, if not completely devoid of, Cl.[15,16] Yet the solar cell devices that use $CH_3NH_3PbI_{3-x}Cl_x$ absorber layers have demonstrated superior charge mobility and lifetimes compared to solar cells made with Cl-free, $CH_3NH_3PbI_3$ absorber layers or other mixed lead halide-based perovskite absorber layers implying that Cl plays a key role in efficiency enhancement.[15,17,18] Recently Edri et al. highlighted the high efficiency with which electrons are transferred across the $CH_3NH_3PbI_{3-x}Cl_x$ perovskite/TiO_2 interface[19] and elucidated the charge carrier separation and working mechanism for $CH_3NH_3PbI_{3-x}Cl_x$ based solar cells, describing it as characteristic of a p-i-n solar cell. You et al. have reported a weak n-type or intrinsic behaviour for a $CH_3NH_3PbI_{3-x}Cl_x$ layer in a glass/ITO/PEDOT:PSS/$CH_3NH_3PbI_{3-x}Cl_x$/PCBM/Al structure[16] whereas Etgar et al. reported p-type behavior for a $CH_3NH_3PbI_3$ perovskite layer.[11] These combined results imply that the p-i-n behaviour suggested by Edri[19] may arise from Cl concentration gradients within the perovskite layer. Surface photovoltage measurements by the Cahen group indicated that the $CH_3NH_3PbI_{3-x}Cl_x/TiO_2$ interface is the dominant interface for photovoltage generation, and that the observed surface photovoltage was a result of changes in band-bending within the absorber layer.[20] Roiati et al. recently demonstrated the existence of oriented permanent dipoles at

Energy & Environmental Science Accepted Manuscript

the $CH_3NH_3PbI_{3-x}Cl_x/TiO_2$ interface and hypothesized that the perovskite layer is highly ordered near the $CH_3NH_3PbI_{3-x}Cl_x/TiO_2$ interface.[21] Recent theoretical calculations by Mosconi et al. showed that the presence of Cl at the perovskite/TiO_2 interface leads to an increased binding strength of the perovskite film to the TiO_2 surface.[22] In turn, this leads to stronger interfacial coupling between the titanium d- and lead p-bands that aids electron injection, increases electron accumulation at the interface, and causes a slight shift in the TiO_2 conduction band to higher energies.[22] Experimental evidence for the presence of Cl at the perovskite/TiO_2 interface in ultra-thin perovskite films (a few nm thick) was recently obtained and supported by DFT calculations.[23] The DFT calculations predicted a chloride-induced band bending at the perovskite/TiO_2 interface that may improve the efficiency of charge collection.[23] Whether this holds true for film thicknesses approaching those used in a device remains unclear. These studies all highlight how the unique properties of $CH_3NH_3PbI_{3-x}Cl_x$ absorber layers and the interface it forms with TiO_2 influence device performance. Some uncertainty remains, however, as to the distribution of Cl within the perovskite layer, if it is present at all, and what role it plays in device performance.

We have conducted X-ray spectroscopic measurements with a variety of information depths to determine the distribution of Cl in $CH_3NH_3PbI_{3-x}Cl_x$ perovskite absorber layers deposited on compact TiO_2. Specifically we have used hard X-ray photoelectron spectroscopy (HAXPES) at different photon energies and fluorescence yield X-ray absorption spectroscopy (FY-XAS) to interrogate the chemical composition of the $CH_3NH_3PbI_{3-x}Cl_x$ perovskite layer from its surface, into its bulk, and through the perovskite layer to the interface formed between the $CH_3NH_3PbI_{3-x}Cl_x$ perovskite and underlying TiO_2. The advantage of using these spectroscopic techniques for depth dependent chemical information over other frequently used techniques (e.g., energy-dispersive X-ray spectroscopy (EDX) and sputtering) is their non-destructive nature which guarantees that the measurement has not modified the chemical composition of the perovskite film. Our results indicate that the surface region is devoid of Cl, within the sensitivity of the employed spectroscopic methods, and that a higher concentration of Cl is present in the deeper half of the perovskite film (i.e., nearer the perovskite/TiO_2 interface than the surface) and perhaps at the $CH_3NH_3PbI_{3-x}Cl_x$ perovskite/TiO_2 interface. The consequences of this distribution of Cl within the $CH_3NH_3PbI_{3-x}Cl_x$ perovskite layer on device performance are discussed.

Experimental

Hard X-ray photoelectron spectroscopy

Hard X-ray photoelectron spectroscopy (HAXPES) experiments were conducted at the HiKE end-station on the KMC-1 beamline of the BESSY-II electron storage ring.[24, 25] This end-station is equipped with a Scienta R4000 electron energy analyzer capable of measuring photoelectron kinetic energies up to 10 keV. A pass energy of 200 eV was used for all measurements. Spectra were recorded with photon energies set to nominal values of 2003 eV and 6009 eV using the first and third diffraction order from a Si(111) double crystal monochromator. Photon energy calibrations using the Au $4f_{7/2}$ peak and the Au Fermi edge consistently show that the true photon energy is within a few eV of the set energy. Below, we simply use 2 and 6 keV to denote the spectra measured with these two photon energies. The combined analyzer plus beamline resolution is better than 0.25 eV for spectra taken at both 2 and 6 keV. The top surface of the sample was grounded for all measurements. The binding energy was calibrated by measuring the 4f spectrum of a grounded Au foil and setting the Au $4f_{7/2}$ binding energy equal to 84.00 eV.

X-ray Absorption Spectroscopy

Cl K-edge fluorescence yield X-ray absorption spectroscopy (FY-XAS) measurements were conducted at the HiKE end-station on the KMC-1 beamline at the BESSY-II electron storage ring using a Bruker XFlash® 4010 silicon drift detector with beryllium window to detect the fluorescence photons. The incident photon energy was scanned from 2814.4 eV to 2844.4 eV (see below for incident photon energy calibration) and Cl K_α fluorescence (at 2618 eV) was detected. To eliminate the detection of elastically scattered photons we collect a relatively narrow photon energy window (approximately 133 eV wide) around 2618 eV when detecting the fluorescence photons. This width is nearly equal to the detector resolution which is estimated to be 132 eV for Mn K_α fluorescence at 5899 eV (Bruker AXS GmbH, Karlsruhe, Germany). The initial photon energy for FY-XAS spectra was calibrated by measuring the kinetic energy of photoelectrons emitted from the Au 4f level of a grounded Au-foil using the first and third diffraction order of the designated initial photon energy. The difference in kinetic energy of the photoelectrons from the Au 4f levels using the first and third diffraction order is equal to twice the photon energy. The photon energy initially set to 2815 eV was calibrated to be 2814.4 eV. This −0.6 eV was used as an offset for the photon energy over the entire spectrum. The X-rays were incident on the sample at an angle of 3.7° from the plane of the sample surface, i.e., grazing incidence. The detection angle was about 45°. The X-rays were horizontally polarized and therefore the polarization vector was nearly normal to the sample surface. The FY-XAS signal was divided by the current measured from an ionization chamber filled with N_2 gas through which the incident beam passed, I_0, which is proportional to the incident photon beam intensity. The spectra were further normalized using the edge jump method.[26]

Sample Preparation

To prepare compact layers of TiO_2 a solution of titanium isopropoxide in ethanol was used. A few drops of diluted hydrochloric acid were added to the precursor solution to make it more stable. The solution was then spin-coated at 2000 rpm for 60 s, dried at 150°C and annealed at 500°C for 45 min.

The solution used for drop-casting the perovskite layer for the annealing experiments was prepared following well established synthesis methods.[6, 10, 27] A solution composed of a 3:1 mixture of CH_3NH_3I:$PbCl_2$ in DMF was drop-cast onto a compact TiO_2 layer on FTO/glass. Following drop-casting the sample was allowed to dry for approximately five minutes before being introduced into the load-lock chamber of the HiKE end-station. Once inside the load-lock chamber the pressure was rapidly pumped down to below 10^{-4} mbar, at which pressure we assume that all the DMF had evaporated. After further evacuation of the load-lock chamber to below 10^{-6} mbar, the sample was transferred into the chamber used for the HAXPES measurements.

The 60 nm (nominal) thick perovskite layer on compact TiO_2 sample was prepared at the University of Oxford by spin-coating the $CH_3NH_3PbI_{3-x}Cl_x$ precursor solution at 2000 rpm in a nitrogen filled glovebox for 45 seconds. After spin-coating, the films were left to dry at room temperature in the glovebox for 30 minutes, to allow slow evaporation of the solvent. They were then annealed to crystallize the perovskite in the glovebox at 90°C for 2.5 hours and then heated to 120°C for 15 minutes. These samples were transferred from the University of Oxford to the BESSY-II synchrotron facility under inert gas. The samples were briefly exposed to air (< 5 min.)

Energy & Environmental Science Accepted Manuscript

 This journal is © The Royal Society of Chemistry 2012

upon introduction into the load-lock chamber of the HiKE end-station. Samples prepared using the same procedure have shown that the perovskite layer coverage is approximately 75 % for 50 nm thick films and approximately 83% for 100 nm thick films.[13] 100 % coverage is difficult to achieve with these films. SEM images further revealed that the incomplete coverage is due to small pores in the otherwise flat film.[13]

Results and Discussion

Figure 1 shows Cl 2p HAXPES spectra taken with a photon energy of 2 keV of a CH_3NH_3I + $PbCl_2$ film (3:1 molar ratio) drop-cast on a compact TiO_2 layer before and after heating in ultra-high vacuum (UHV) to 140 °C. The initially deposited, unannealed film shows a strong Cl 2p signal indicative of Cl in the surface region of the film. The binding energy of the Cl $2p_{3/2}$ peak is 197.6 eV and is consistent with the Cl $2p_{3/2}$ binding energies observed for metal chlorides.[28] We estimate that spectra taken with photon energies of 2 keV have an

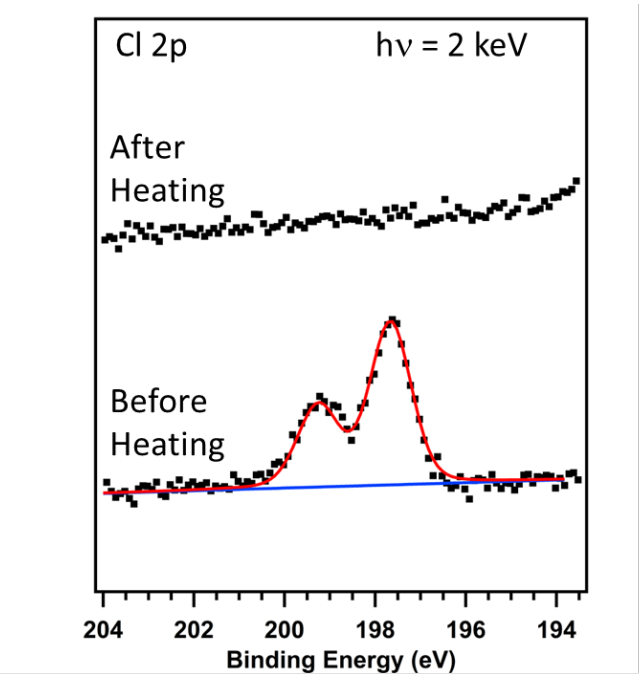

Figure 1: Cl 2p spectra taken with a photon energy of 2 keV of a 3 : 1 mole ratio, CH_3NH_3I : $PbCl_2$, solution in DMF, drop-cast onto a compact TiO_2 layer and dried in UHV; at room temperature before heating (bottom), after heating to 140 °C (top).

information depth of approximately 10 nm (cf. S.I.). The Cl 2p spectrum in Figure 1 shows that, after annealing the sample, the concentration of Cl in the top 10 nm of the perovskite film has drastically decreased to a level where it can no longer be detected. We estimate that the concentration ratio of Cl to I in the surface region must be less than approximately 0.024 (cf. S.I.), notably lower than the Cl : I concentration ratio of the initial solution (0.66). We also note that *in-situ* monitoring of the Cl 2p signal during annealing indicates that the Cl concentration in the surface region of the film begins to decrease at relatively low temperatures and has already fallen below the detection limit by temperatures of about 50 °C (cf. S.I.).

As to what happens to the Cl, there are a few possibilities. Since our measurements are conducted under UHV conditions it is possible that Cl desorbs from the film and is pumped away as Cl_2(g) or CH_3NH_3Cl(g) during annealing of the perovskite film thereby depleting the surface region of the film of Cl.[29] Note that this may also occur when annealing perovskite films in air or in inert atmospheres, since Cl_2 is a gas at ambient conditions. The rate of Cl depletion will depend on the rates of diffusion of Cl through the perovskite layer and Cl_2 or CH_3NH_3Cl formation and desorption. Such a process would likely be very sensitive to annealing conditions, including both temperature and time. Another possibility is that as the film is annealed and the perovskite structure is formed the Cl diffuses more deeply into the bulk of the film (i.e., towards the $CH_3NH_3PbI_{3-x}Cl_x/TiO_2$ interface) thereby depleting the surface region of Cl and increasing the Cl concentration deeper within the film. It is also possible that a combination of these mechanisms occurs, i.e., some Cl is lost to the gas phase and some diffuses deeper into the film as the perovskite layer is formed.

To determine if Cl is located deeper in the film we have conducted photoelectron spectroscopy with multiple photon energies of a 60 nm thick perovskite film deposited on a compact TiO_2 layer. The photon energies used were 2 keV and 6 keV. The use of higher photon energies increases the inelastic mean free path (IMFP) of the photoelectrons emitted from a specific core level and therefore increases the information depth of the measurement. We estimate that the information depths for spectra taken with 2 and 6 keV are approximately 10 nm and 26 nm respectively (cf. S.I.). Figure 2 shows the Cl 2p and I 4s region of the 60 nm thick perovskite film taken with these two photon energies. Again, neither spectrum shows the presence of Cl. Due to a change in the relative photoionization cross-sections of the Cl 2p and I 4s levels the minimum amount of detectable Cl relative to I is higher (Cl : I < 0.15, cf. S.I.) for 6 keV excitation than the value for 2 keV excitation (Cl : I < 0.024). Considering the chemical formula for the perovskite, $CH_3NH_3PbI_{(3-x)}Cl_x$, the concentration ratio of Cl : I is equal to x/(3-x). Using our maximum possible values of the Cl : I ratio we can estimate a maximum possible value of x from the data taken at the two photon energies. This value is 0.07 for the 2 keV spectra and 0.40 for the 6 keV spectra. Combining this with our estimated information depth and assuming a homogeneous

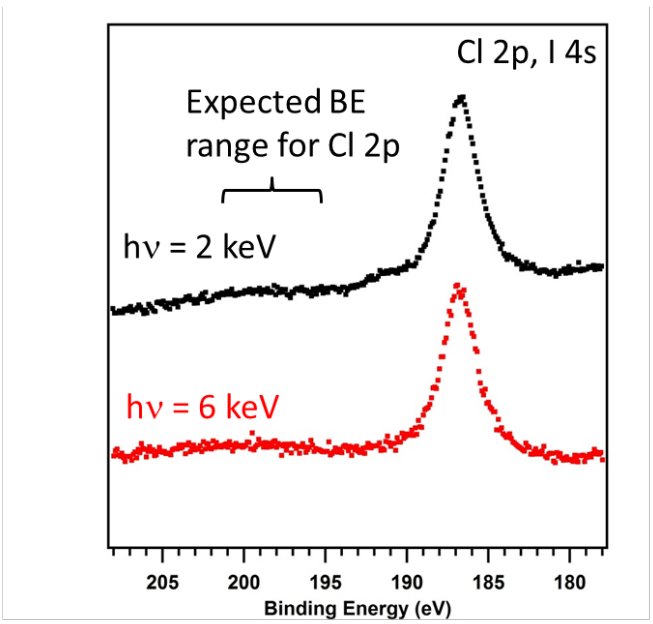

Figure 2: Cl 2p and I 4s spectra taken with a photon energies of 2 keV (black) and 6 keV (red) of a 60 nm thick $CH_3NH_3PbI_{3-x}Cl_x$ film on compact TiO_2. Note the absence of any detectable Cl in both spectra.

Energy & Environmental Science Accepted Manuscript

distribution of Cl to this depth we find that x < 0.07 up to 10 nm deep into the perovskite film and x < 0.40 up to 26 nm deep into the perovskite film. Note again that the difference in the upper limit for x at the two different depths is due to differences in the detection limit of Cl at the two different photon energies (caused by different photoionization cross sections) as discussed above and does not confirm or exclude the possibility of a Cl concentration gradient, with a Cl concentration below the detection limit, throughout the near-surface region of the perovskite film.

The information depth of photon-in / photon-out spectroscopic techniques, such as fluorescence yield X-ray absorption spectroscopy (FY - XAS), is determined by the attenuation length of the photons through the material of interest.[30] The attenuation lengths of soft X-ray photons are typically much larger than the IMFPs of the photoelectrons of XPS and HAXPES in most materials. We have taken advantage of the increased information depth of FY-XAS compared to HAXPES in an attempt to detect Cl throughout the entire 60 nm thick perovskite film. In our experiments the angle between the detector and the sample surface (~45°) is much larger than the angle between the incident X-rays and the sample surface (3.7°), and so the information depth for the FY-XAS spectra is determined by the depth of penetration of the incident photons beneath the sample surface. We have calculated that the information depth for our FY-XAS measurements is approximately 100 nm (cf. S.I.).[31] Therefore, in our FY-XAS measurements, we are approximately sampling the entire 60 nm thick perovskite film and the top 40 nm portion of the compact TiO_2 layer underneath.

Figure 3 shows Cl K-edge FY-XAS spectra for the 60 nm $CH_3NH_3PbI_{(3-x)}Cl_x$ perovskite film on top of a compact TiO_2 layer (blue) and of a compact TiO_2 layer without any perovskite film (green). In both cases we observe Cl K-absorption in the spectra however the shapes of the two spectra differ. The Cl K-edge spectrum of the perovskite/TiO_2 sample is composed of three broad features located at ~ 2824.7 eV, 2827.4 eV, and 2832.3 eV, whereas the Cl K-edge spectrum of the TiO_2 without the perovskite layer is dominated by two peaks located at ~ 2824.1 eV and ~ 2832.5 eV and a broad lower intensity shoulder between these two peaks located at ~ 2829.2 eV. The differences in the two spectra shown in Figure 3 reflect the fact that most of the Cl observed in the perovskite/TiO_2 sample has different local bonding than the Cl in the compact TiO_2 layer.[26] The spectra in Figure 3 provide direct evidence for the presence of Cl deep within the perovskite film. The Cl K-absorption observed in the spectrum of the bare TiO_2 film is likely due to residual Cl from the solution used to deposit the TiO_2 film (cf. Experimental section). Further, comparing the FY-XAS spectrum of the perovskite/TiO_2 sample to previously published FY-XAS spectra of $PbCl_2$, indicates that the local bonding of the Cl observed in the perovskite/TiO_2 sample also differs from that found in $PbCl_2$.[32] The FY-XAS measurements are bulk sensitive and probe the entire thickness of the perovskite film and, as a result, we attribute the $CH_3NH_3PbI_{(3-x)}Cl_x/TiO_2$ Cl-K edge spectrum (Figure 3, blue) to Cl deep within the perovskite layer. Since the Cl K edge FY-XAS measurements indicate that x > 0.40 on average throughout the perovskite film (cf. S. I.) and our HAXPES measurements indicate that x < 0.40 in the top 26 nm of the film, there must be an enhanced concentration of Cl within the bottom half of the perovskite film (i.e., nearer the perovskite/TiO_2 interface than the surface) or at the $CH_3NH_3PbI_{(3-x)}Cl_x/TiO_2$ interface. We cannot entirely exclude that the Cl in the TiO_2 layer (green) also contributes a small amount to the spectrum of the $CH_3NH_3PbI_{(3-x)}Cl_x/TiO_2$ sample, but it is apparent that its overall shape differs considerably. We are currently conducting more detailed experiments to understand the local bonding of the Cl deep within the perovskite layer.

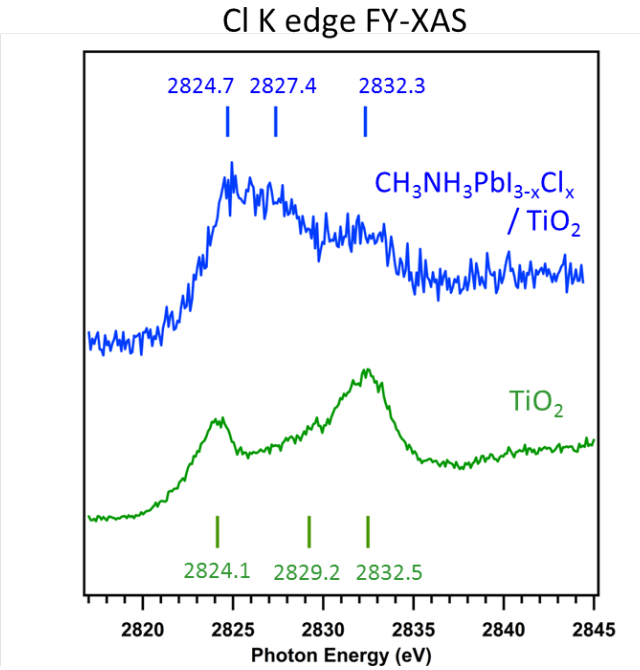

Figure 3: Cl K edge FY-XAS spectra of a 60 nm thick $CH_3NH_3PbI_{3-x}Cl_x$ layer on compact TiO_2 (blue) and the compact TiO_2 layer without a $CH_3NH_3PbI_{3-x}Cl_x$ layer on top (green). Note the distinctively different shapes of the two spectra.

We note that we could not unambiguously detect the presence of Cl in the perovskite layer with Cl K edge FY-XAS in all $CH_3NH_3PbI_{(3-x)}Cl_x/TiO_2$ samples that we have analysed. The variation in interfacial Cl content from sample to sample likely indicates that it is very sensitive to processing conditions, in particular annealing temperature and time. However, the combined observations of Cl deep in the $CH_3NH_3PbI_{(3-x)}Cl_x$ film or at the $CH_3NH_3PbI_{(3-x)}Cl_x/TiO_2$ interface and lack of Cl in the surface or near-surface region for most samples point to an increased stability of the Cl in the bottom half of $CH_3NH_3PbI_{(3-x)}Cl_x$ layers on compact TiO_2 compared to the surface and near-surface regions. Since Cl plays a beneficial role in $CH_3NH_3PbI_{(3-x)}Cl_x$ – based solar cell devices,[15,17,18] optimizing the processing conditions for maximum benefit from this Cl distribution is likely key to further enhance device efficiency and achieve device performance consistency.

To summarize, our results indicate that the concentration of Cl is higher (x > 0.40) in the bottom half of the perovskite film or in the proximity of the perovskite/TiO_2 interface than in the top half of the perovskite film. In addition, our HAXPES measurements provide an upper limit to the amount of Cl present to certain depths in the perovskite film: x < 0.07 up to 10 nm, and x < 0.40 up to 26 nm deep beneath the surface of the $CH_3NH_3PbI_{(3-x)}Cl_x$ perovskite layer and our FY-XAS measurements indicate x > 0.40 for depths greater than 26 nm beneath the surface of the perovskite film. Note however, that Cl may still be present at very low concentrations near the surface and throughout the bulk of the perovskite layer. We now discuss potential consequences of this distribution of Cl in the perovskite layer.

The precise role of Cl in the perovskite layer remains unclear, but understanding its location allows us to speculate about a few possibilities. The presence of Cl deep within the perovskite layer may affect both the structural and electronic properties of the perovskite/TiO_2 interface. Surface science studies and ab initio calculations of Cl adsorption on TiO_2(110) indicate that Cl adsorbs

Energy & Environmental Science Accepted Manuscript

This journal is © The Royal Society of Chemistry 2012

at both oxygen vacancy defects and regular Ti^{4+} sites on the surface at room temperature with the oxygen vacancy defect sites being more stable.[33,34] These studies also indicated that at moderate temperatures (initially starting at 120 °C) the Cl can replace some of the oxygen on the surface and reduce neighbouring Ti-sites from Ti^{4+} to Ti^{3+}. (Note that Cl only needs one electron to form a complete shell, whereas oxygen needs two. The extra electron when Cl replaces O is left to reduce the neighbouring Ti^{4+}.) The presence of Cl may lead to improved electronic properties of the perovskite/TiO2 interface in multiple ways. The present study suggests that if the Cl observed in the FY-XAS measurements is located at the perovskite/TiO_2 interface this may quench oxygen vacancy defect states that act as charge traps in the band gap of the TiO_2 surface, and facilitate charge transfer across the interface. Further, previous surface science studies also suggested that a defect-mediated process may be responsible for the replacement of oxygen in the TiO_2 surface by Cl.[34] In this mechanism, Ti interstitials and oxygen vacancies migrate from the near-surface region of the TiO_2 to the surface where they react with Cl. Such a mechanism may be a driving force that causes Cl segregation to and stabilization at the perovskite TiO_2 interface upon annealing the perovskite film. This would also decrease the number of charge trap states in the near-interface region of the TiO_2 at the perovskite/TiO_2 interface and be consistent with the results of Mosconi et al. who found higher electron injection efficiencies when Cl is present at the interface.[22] Cl located at the perovskite/TiO_2 interface may also induce band bending and improve charge collection efficiency of the electron-selective contact, TiO_2.[23]

In addition to enhancing the electronic properties of the perovskite/TiO_2 interface region, the presence of Cl may provide a better template for perovskite film growth leading to less disorder in $CH_3NH_3PbI_{3-x}Cl_x$ perovskite films compared to Cl-free $CH_3NH_3PbI_3$ films. Alluding to this are recent theoretical calculations by Mosconi et al. showing that the presence of Cl at the perovskite/TiO_2 interface increases the stability of [110] oriented films, the preferred orientation for perovskite film growth on TiO_2, leading to better film crystallinity as a result of a templating-like mechanism.[22] In turn, a more highly ordered perovskite film may result in more favourable electronic properties of the perovskite layer. A more defect-free perovskite layer would likely provide a better layer for charge transport than a highly defective layer.[21] If this is the case, the interfacial Cl induced crystallinity suggested by Mosconi et al.[22] may help to explain the much longer electron and hole diffusion lengths for mixed halide perovskite layers ($CH_3NH_3PbI_{3-x}Cl_x$) compared to tri-iodide perovskite layers ($CH_3NH_3PbI_3$).[17,18] However, a similar Cl-templating mechanism would also have to act at the $CH_3NH_3PbI_{3-x}Cl_x$/glass interface.[17] A Cl-templating mechanism would not play as large a role in device structures using nano-structured TiO_2, since they do not require as long electron and hole diffusion lengths. This may help to explain the observed efficiencies of devices made with Cl-free, $CH_3NH_3PbI_3$ absorber layers when combined with nano-structured TiO_2.[10,11] Lastly, the much longer diffusion lengths in $CH_3NH_3PbI_{3-x}Cl_x$ perovskite layers may also be explained by low levels of Cl remaining throughout the perovskite layer (below the detection levels of HAXPES) that act as a dopant and facilitate charge transport.[15]

Our results may also help to explain the p-i-n behavior of $CH_3NH_3PbI_{3-x}Cl_x$ solar cell layers suggested by Edri.[19] Locations in the layer of high Cl concentration (i.e., deeper in the perovskite layer, nearer the perovskite/TiO_2 interface as demonstrated here) have n-type character,[16] whereas those areas of little or no Cl (i.e., the surface and near-surface region of the perovskite layer in our current study, or the perovskite/HTM (hole transport material) interface in a device) have p-type character.[11] This may lead to p-i-n type behaviour in the film. We note however that more work is required to understand the electronic consequences of the physical location of the chlorine although rapid progress is being made in this respect.[11,16,19–22]

Conclusion

HAXPES measurements using different photon energies have demonstrated that the surface and near surface regions of a $CH_3NH_3PbI_{3-x}Cl_x$ layer on compact TiO_2 are Cl depleted. The detection limit of the HAXPES measurements allows us to put an upper limit on the amount of Cl in the perovskite film as a function of depth beneath the surface of the perovskite film. To depths of ~10 nm, $x < 0.07$ and to depths of ~26nm, $x < 0.40$ in the chemical formula for the perovskite: $CH_3NH_3PbI_{3-x}Cl_x$. Cl K-edge FY-XAS, however, has revealed that, if present, the concentration of Cl is enhanced deep in the perovskite film perhaps at or near the $CH_3NH_3PbI_{3-x}Cl_x/TiO_2$ interface. The distribution of Cl within the perovskite layer is likely to be an important factor for understanding and optimizing the function of $CH_3NH_3PbI_{3-x}Cl_x$ mixed-halide perovskite based solar cells. Being able to control and manipulate the Cl distribution may provide a means to improve $CH_3NH_3PbI_{3-x}Cl_x$-based solar cell device performance through graded electronic properties.

Acknowledgements

DES, EH, RGW, JHA, LK, and MB gratefully acknowledge the Impuls- und Vernetzungsfonds of the Helmholtz-Association (VH-NG-423) for financial support.

Notes

[a]*Renewable Energy, Helmholtz-Zentrum Berlin für Materialien und Energie GmbH, D-14109 Berlin, Germany*
[b]*Department of Physics, Clarendon Laboratory, University of Oxford, Oxford, OX1 3PU, UK*
[c]*Energy Materials In-Situ Laboratory Berlin (EMIL), Helmholtz-Zentrum Berlin für Materialien und Energie GmbH, D-12489 Berlin, Germany*
[d]*Institute for Methods and Instrumentation for Synchrotron Radiation Research, Helmholtz-Zentrum Berlin für Materialien und Energie GmbH, D-12489 Berlin, Germany*
[e]*Institut für Physik und Chemie, Brandenburgische Technische Universität Cottbus-Senftenberg, D-03046 Cottbus, Germany*

**Corresponding authors: david.starr@helmholtz-berlin.de*
h.snaith1@physics.ox.ac.uk

† Electronic Supplementary Information (ESI) available: Estimation of information depth for HAXPES measurements, estimation of Cl detection limit, evidence for Cl 2p signal falling below the detection limit by 50 °C and estimation of Cl K edge FY-XAS Cl detection limit. See DOI: 10.1039/b000000x/

References

1 Wolden, C. A.; Kurtin, J.; Baxter, J. B.; Repins, I.; Shaheen, S. E.; Torvik, J. T.; Rockett, A. A.; Fthenakis, V. M.; Aydil, E. S. Photovoltaic Manufacturing: Present Status, Future Prospects, and Research Needs. *J. Vac. Sci. Technol. A* **2011**, *29*, 030801.

Energy & Environmental Science Accepted Manuscript

2 Peter, L. M. Towards Sustainable Photovoltaics: The Search for New Materials. *Phil. Trans. R. Soc.* **2011**, *369*, 1840 – 1856.
3 Branker, K.; Pathak, M. J. M.; Pearce, J. M. A Review of Solar Photovoltaic Levelized Cost of Electricity. *Renewable and Sustainable Energy Reviews* **2011**, *15*, 4470 – 4482.
4 Hegedus, S. *Prog. Photovolt: Res. Appl.* **2006**, *14*, 393 – 411.
5 Kojima, A.; Teshima, K.; Shirai, Y.; Miyasaka, T. Organometal halide perovskites as visible.light sensitizers for photovoltaic cells. *J. Am. Chem. Soc.*, **2009**, *131*, 6050 – 6051.
6 Zhou, H.; Chen, Q.; Li, G.; Luo, S.; Song, T.-B.; Duan, H.-S.; Hong, Z.; You, J.; Liu, Y.; Yang, Y. Interface engineering of highly efficient perovskite solar cells. *Science*, **2014**, 345, 542 – 546.
7 "Best Research-Cell Efficiencies" chart compiled by the National Center for Photovoltaics at the National Renewable Energy Laboratory, Golden, CO, U.S.A., http://www.nrel.gov/ncpv/, last accessed March 27, 2015.
8 Snaith, H. J. Perovskites: The Emergence of a New Era for Low-Cost, High Efficiency Solar Cells. *J. Phys. Chem. Lett.* **2013**, *4*, 3623 – 3630.
9 Liu, M.; Johnston, M. B.; Snaith, H. J. Efficient Planar Heterojunction Perovskite Solar Cells by Vapour Deposition. *Nature* **2013**, *501*, 395 – 398.
10 Burschka, J.; Pellet, N.; Moon, S. –J.; Humphry-Baker, R.; Gao, P.; Nazeeruddin, M. K.; Grätzel, M. Sequential Deposition as a Route to High-Performance Perovskite-Sensitized Solar Cells. *Nature* **2013**, *499*, 316 – 319.
11 Etgar, L.; Gao, P.; Xue, Z.; Peng, Q.; Chandiran, A. K.; Liu, B.; Nazeeruddin, M. K.; Grätzel, M. Mesoscopic $CH_3NH_3PbI_3/TiO_2$ Heterojunction Solar Cells. *J. Am. Chem. Soc.* **2012**, *134*, 17396 – 17399.
12 Docampo, P.; Ball, J. M.; Darwich M.; Eperon, G. E.; Snaith, H. J. Efficient Organometal Trihalide Perovskite Planar-Heterojunction Solar Cells on Flexible Polymer Substrates. *Nature Comm.* **2013**, *4*, 2761.
13 Eperon, G. E.; Burlakov, V. M.; Docampo, P.; Goriely, A.; Snaith, H. J. Morphological Control for High Performance, Solution-Processed Planar Heterojunction Perovskite Solar Cells. *Adv. Funct. Mater.* **2014**, *24*, 151 – 157.
14 Baikie, T.; Fang, Y.; Kadro, J. M.; Schreyer, M.; Wie, F.; Mhaisalkar, S. G.; Graetzel, M.; White, T. J. Synthesis and Crystal Chemistry of the Hybrid Perovskite $(CH_3NH_3)PbI_3$ for Solid-State Sensitised Solar Cell Applications. *J. Mater. Chem. A* **2013**, *1*, 5628 – 5641.
15 Colella, S.; Mosconi, E.; Fedeli, P.; Listorti, A.; Gazza, F.; Orlandi, F.; Ferro, P.; Besgni, T.; Rizzo, A.; Calestani, G.; Gigli, G.; De Angelis, F.; Mosca, R. $MAPbI_{3-x}Cl_x$ Mixed Halide Perovskite for Hybrid Solar Cells: The Role of Chloride as Dopant on the Transport and Structural Properties. *Chem. Mater.* **2013**, *25*, 4613 – 4618.
16 You, J.; Hong, Z.; Yang, Y.; Chen, Q.; Cai, M.; Song, T.-B.; Chen, C.-C.; Lu, S.; Liu, Y.; Zhou, H.; Yang, Y. Low-Temperature Solution-Processed Perovskite Solar Cells with High Efficiency and Flexibility. *ACS Nano* **2014**, *8*, 1674 – 1680.
17 Stranks, S. D.; Eperon, G. E.; Grancini, G.; Menelaou, C.; Alcocer, M. J. P.; Leijtens, T.; Herz, L. M.; Petrozza, A.; Snaith, H. J. Electron-Hole Diffusion Lengths Exceeding 1 Micrometer in an Organometal Trihalide Perovskite Absorber *Science* **2013**, *342*, 341 – 344.
18 Xing, G.; Mathews, N.; Sun, S.; Lim, S. S.; Lam, Y. M.; Grätzel, M.; Mhaisalkar, S.; Sum, T. C. Long-Range Balanced Electron- and Hole-Transport Lengths in Organic-Inorganic $CH_3NH_3PbI_3$ *Science* **2013**, *342*, 344 – 347.
19 Edri, E.; Kirmayer, S.; Mukhopadhyay, S.; Gartsman, K.; Hodes, G.; Cahen, D. Elucidating the Charge Carrier Separation and Working Mechanism of $CH_3NH_3PbI_{3-x}Cl_x$ Perovskite Solar Cells. *Nature Comm.* **2014**, *5*, 3461.
20 Barnea-Nehoshtan, L.; Kirmayer, S.; Edri, E.; Hodes, G.; Cahen, D. Surface Photovoltage Spectroscopy Study of Organo-Lead Perovskite Solar Cells. *J. Phys. Chem. Lett.* **2014**, *5*, 2408 – 2413.
21 Roiati, V.; Mosconi, E.; Listorti, A.; Colella, S.; Gigli, G.; De Angelis, F. Stark Effect in Perovskite/TiO_2 Solar Cells : Evidence of Local Interfacial Order. *Nano Lett.* **2014**, *14*, 2168 – 2174.
22 Mosconi, E.; Ronca, E.; De Angelis, F. First-Principles Investigation of the TiO_2/Organohalide Perovskites Interface : The Role of Interfacial Chlorine. *J. Phys. Chem. Lett.* **2014**, *5*, 2619 – 2625.
23 Colella, S.; Mosconi, E.; Pellegrino, G.; Alberti, A.; Guerra, V. L. P.; Masi, S.; Listorti, A.; Rizzo, A.; Condorelli, G. G.; De Angelis, F.; Gigli, G. Elusive Presence of Chloride in Mixed Halide Perovskite Solar Cells. *J. Phys. Chem. Lett.* **2014**, *5*, 3532 – 3538.
24 Gorgoi, M.; Svensson, S.; Schäfers, F.; Öhrwall, G.; Mertin, M.; Bressler, P.; Karis, O.; Siegbahn, H.; Sandell, A.; Rensmo, H.; Doherty, W.; Jung, C.; Braun, W.; Eberhardt, W. The High Kinetic Energy Photoelectron Spectroscopy Facility at BESSY Progress and First Results. *Nucl. Instrum. Methods A* **2009**, *601*, 48 – 53.
25 Schaefers, F.; Mertin, M.; Gorgoi, M. KMC-1: A High Resolution and High Flux Soft X-ray Beamline at BESSY. *Rev. Sci. Instrum.* **2007**, *78*, 123102.
26 Stöhr, J. *NEXAFS Spectroscopy*; Springer-Verlag: Berlin, Germany, 2003.
27 Ball, J. M.; Lee, M. M.; Hey, A.; Snaith, H. J. Low-Temperature Processed Meso-Superstructured to Thin-Film Perovskite Soalr Cells. *Energy Environ. Sci.* **2013**, *6*, 1739 – 1743.
28 NIST X-ray Photoelectron Spectroscopy Database, Version 4.1 (National Institute of Standards and Technology, Gaithersburg, 2012); http://srdata.nist.gov/xps/.
29 Yu, H; Wang, F.; Xie, F.; Li, W.; Chen, J.; Zhao, N. The Role of Chlorine in the Formation Process of $CH_3NH_3PbI_{3-x}Cl_x$. *Adv. Funct. Mater.* **2014**, *24*, 7102 – 7108.
30 De Groot F.; Kotani, A. *Core Level Spectroscopy of Solids;* CRC Press: Boca Raton, FL, USA, 2008.
31 Henke, B. L.; Gullikson, E. M.; Davis, J. C. X-ray Interactions: Photoabsorption, Scattering, Transmission, and Reflection at E = 50 – 30000 eV, Z = 1 – 92. *Atomic Data and Nuclear Data Tables* **1993**, *54*, 181 – 342.
32 Sugiura, C.; Nakai, S.-I. X-ray Spectroscopic Investigation of Lead Chloride, $PbCl_2$. *Phys. Rev. B* **1983**, *28*, 1088 – 1092.
33 Hebenstreit, E. L. D.; Hebenstreit, W.; Geisler, H.; Ventrice Jr., C. A.; Hite, D. A.; Sprunger, P. T.; Diebold, U. The Adsorption of Chlorine on TiO_2(110) Studied with Scanning Tuneling Microscopy and Photoemission Spectroscopy. *Surf. Sci.* **2002**, *505*, 336 – 348.

Energy & Environmental Science Accepted Manuscript

This journal is © The Royal Society of Chemistry 2012

34 Vogtenhuber, D.; Podloucky, R.; Redinger, J. Ab Initio Study of Atomic Cl Adsorption on Stoichiometric and Reduced Rutile TiO_2(110) Surfaces. *Surf. Sci.* **2000**, *454 – 456*, 369 – 373.

Energy & Environmental Science Accepted Manuscript

T. O. C. Graphics

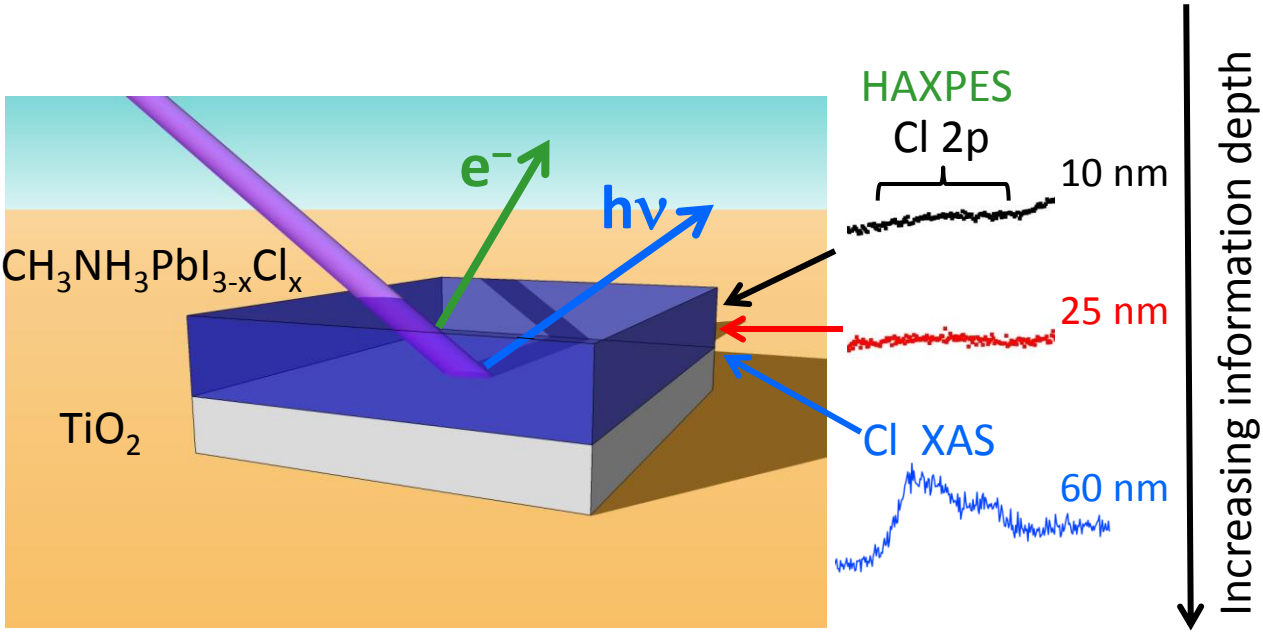

Caption: X-ray spectroscopies have shown a higher chlorine concentration near the perovskite/TiO_2 interface than throughout the rest of the perovskite film.

Energy & Environmental Science Accepted Manuscript

David E. Starr et al., Manuscript ID EE-ART-02-2015-000403

"Direct Observation of an Inhomogeneous Chlorine Distribution in $CH_3NH_3PbI_{3-x}Cl_x$ Layers: Surface Depletion and Interface Enrichment"

Broader context:

Solution processed, thin-film solar cell technologies promise significant cost reductions for sunlight-to-electricity conversion compared to crystalline silicon-wafer based technology. Thin-film organic-inorganic perovskite-based devices have recently demonstrated dramatic increases in efficiency. Optimal performance for these devices has been achieved with methyl ammonium lead halide absorbers using a mixture of chlorine and iodine. Despite typical chlorine-to-iodine concentration ratios of 0.66 in the initial precursor solution, following deposition onto TiO_2 and processing the perovskite films contain little or no chlorine. An important step towards understanding the apparent beneficial effects of the chlorine is to know where the chlorine is located within the perovskite thin film. Using non-destructive, X-ray spectroscopies to investigate the depth dependent chemical composition of chlorine and iodine containing mixed halide perovskite films, we have observed a higher concentration of chlorine near the perovskite/TiO_2 interface than in the rest of the thin film. With this information in hand, optimization of the Cl-distribution in the perovskite layer via precisely controlled deposition and processing procedures may lead to further improvement in device efficiencies.

Energy & Environmental Science Accepted Manuscript